Open Journal of Applied Sciences, 2022, 12, 1577-1594
https://www.scirp.org/journal/ojapps
ISSN Online: 2165-3925
ISSN Print: 2165-3917

Comparative Study of Zamzam, Bottled Drinking and Distilled Waters by a Novel Computer Simulation Speckle Photography Method Using Fourier Transform

Nasser A. Moustafa[1,2], Hasan Assaedi[2], Thamer H. Albaqami[2]

[1]Physics Department, Faculty of Science, Helwan University, Cairo, Egypt
[2]Physics Department, Teachers Colleges of Makkah, Umm-Al-Qura University, Mecca, Mecca Province, KSA
Email: nasseramoustafa@gmail.com

How to cite this paper: Moustafa, N.A., Assaedi, H. and Albaqami, T.H. (2022) Comparative Study of Zamzam, Bottled Drinking and Distilled Waters by a Novel Computer Simulation Speckle Photography Method Using Fourier Transform. *Open Journal of Applied Sciences*, **12**, 1577-1594.
https://doi.org/10.4236/ojapps.2022.129107

Received: August 7, 2022
Accepted: September 25, 2022
Published: September 28, 2022

Abstract

The refractive index of a liquid medium is an important optical parameter since it exhibits the optical properties of the liquid. Its values are often required to interpret various types of spectroscopic data. The intensity distribution and contrast of image speckle patterns obtained for Zamzam, bottled drinking and distilled waters are investigated on a computer as a function of six discrete wavelengths across the visible spectrum. The present novel computer simulation speckle photography using Fourier transform study and the new theoretical background have been confirmed with previous experimental results. Uncertainty of refractive index measurements was studied on a wide range of discrete wavelengths using the computer simulation and the new theoretical formulae.

Keywords

Zamzam Water, Speckle Photography, Measurement Uncertainty, Comparative Measurement

1. Introduction

Speckle appears when a rough surface is coherently illuminated. Sometimes this is an undesired phenomenon, but it is also extensively exploited in a special class of optical methods: speckle metrology. Speckle based methods are used to characterize surfaces in terms of statistical quantities related to their microscopic features [1]. Computer simulation is a great tool for studying speckle and to design new experimental setups.

H. Fujii, J. Uozumi, and T. Asakura [2] described the intensity distribution and contrast of image speckle patterns for various objects having different surface profiles which investigated on a computer as a function of the surface roughness properties of the objects and the point spread of an imaging system. The computer simulation study for the objects having a random surface gives a theoretical background for the experimental results obtained by Fujii and Asakura [3]. The same study for the objects having a periodic surface of two different profiles indicates that the contrast variation takes a complicated form as a function of the point spread of the imaging system, while the intensity distribution of images simply follows a periodic variation. It becomes clear from the simulation study that the maximum value of the image contrast variation is dependent mainly on the rms surface roughness of the objects but not on their surface profile.

The refractive index of a medium is an important optical parameter since it exhibits the optical properties of the medium. The adulteration problem is increasing day by and hence simple, automatic and accurate measurement of the refractive index of materials is of great importance these days. Quick measurements of refractive indices using simple techniques and refractometers can help controlling adulteration of liquids of common use to a greater extent. Several researchers have used various methods and techniques for the measurement of refractive indices of liquids. Sensitive determination of the refractive indices of certain materials is very important in many fields of research such as material analysis and environmental pollution monitoring.

Chandra and Bhaiya [4] described a very simple method based on the minimum deviation and Snell's law for the determination of refractive indices of various liquids up to the second decimal. They used a hollow prism and kept the angle of incidence constant and measured the angle of deviation.

Jenkins [5] proposed a method using a laser for the measurement of variations in the refractive indices due to the change in concentration of a solution. Recently a very simple method for measuring the refractive index of liquid is presented [6], when a laser beam impinges obliquely on a rectangular cell filled with liquid and passes through the cell, the propagation axis of the transmitted beam is displaced from that of the incident beam. By measuring the displacement, the refractive index of the liquid can be determined. Beams of a He-Ne laser and a laser diode were used for measuring the refractive indices of pure water and some organic liquids.

Rahman [7] studied the variations of refractive index using the method of Bass and Weidner [8] for the case when the concentration of a solution is altered from distilled water to a saturated condition. They measured the refractive indices of liquid solutions at the He-Ne laser wavelength using the conventional minimum deviation method of an equilateral hollow glass prism. This method was identical to that described by Jenkins [5] except that instead of a screen, a telescope was used to find the minimum angle of deviation.

S. Y. El-Zaiat [9] measured the refractive indices of Zamzam water samples by an Abbe refractometer at six discrete wavelengths across the visible spectrum. Some related optical parameters such as: group refractive index; permittivity; specific refraction; polarizability; reflectance; and transmittance have been deduced. Dispersion of these optical parameters across the visible spectrum has been calculated. For comparison, these optical parameters have been determined for two samples of bottled drinking and distilled waters. Also the Abbe number and the single oscillator constants for the three waters have been calculated. Error analyses of the measured and the calculated optical parameters have been given. It has been concluded that Zamzam water has special optical parameters that are different than those of bottled drinking and distilled waters.

Nasser A. Moustafa [10] [11], extended the application of Fourier transform method to speckle photography, to measure the refractive index and thickness of the transparent plate, and detect the major uncertainty components for improving the performance of the refractive index and thickness estimation.

Nasser A. Moustafa [12], proposed a method which is a comparative digital speckle pattern interferometry. This method depends on the comparative study of the computer simulation speckle pattern and the real experiments for analyzing the difference correlation fringes that coexist with the sum correlation fringes, which recorded as a result of the direct optical comparison of two nominally identical objects (master and test). The resultant interference patterns are related to the difference in deformation, shape or refractive index change of the two objects.

In the present work, we used the computer simulation to design an experimental setup for the investigation of the intensity distribution and contrast of image speckle patterns obtained for Zamzam, bottled drinking and distilled waters as a function of six discrete wavelengths across the visible spectrum. The discovered novel computer simulation speckle photography method using Fourier transform study and the new theoretical formulae have been proven with the experimental results obtained by S. Y. El-Zaiat *et al.*, [1]. Uncertainty of refractive index measurements were studied on a wide range of discrete wavelengths using the computer simulation and the new theoretical formulae.

2. Theoretical Background

To measure the refractive index of a liquid, it is putted between two thin glass slides. Spatially coherent light transmitted through the system of the two glass slides and the liquid which in between, and illuminate a rough surface. The obtained speckle is recorded twice, one before changing the angle of incidence of the laser beam and one after given an angle of incidence. The two images are combined digitally "added or subtracted". The resultant image will contain a pair of identical speckle pattern separated by a distance $\Delta\xi$. The displacement $\Delta\xi$ is displaced in the form of fringe pattern by applying FFT to the resultant image. So a bright spot surrounded by a speckle pattern modulated by a correlation fringes can be observed.

Figure 1, shows the propagation of the incident plane wave through the system of the two glass slides and the liquid. The thicknesses of the two glass slides are d_1 and d_3 respectively, also the thickness of the liquid is d_2. The incident plane wave continuous to propagate as a plane wave with wavenumbers k_1, k_2, and k_3 respectively. So the complex amplitude transmittance through the shown system is $t_1(x,y)$, $t_2(x,y)$, and. $t_3(x,y)$ respectively.

Where, $t_1(x,y)=\exp(-jk_1d_1)$, $t_2(x,y)=\exp(-jk_2d_2)$, and $t_3(x,y)=\exp(-jk_3d_3)$.

So the complex amplitude transmittance of the shown system at the normal incidence of the laser beam is as follow,

$$t(x,y)=\exp(-jk_1d_1)\exp(-jk_2d_2)\exp(-jk_3d_3) \tag{1}$$

The amplitude distribution after the first exposure in the observation plane is given as

$$A_1(x,y)=\frac{1}{j\lambda z}a\mathrm{e}^{i\phi}\mathrm{e}^{jkz}\mathrm{e}^{-i(k_1d_1+k_2d_2+k_3d_3)}\mathrm{e}^{\frac{j\pi}{\lambda z}\left(x^2+y^2\right)}F\left\{A(\xi,\eta)\right\} \tag{2}$$

If the incident plane wave makes an angle θ with the x-axis of the system, and transmitted through the first glass slid which has a thickness d_1. The incident and refracted waves are plane waves with wavenumbers k, and k_1, and angles θ and θ_1. Where θ_1 is the angle of refraction through the first glass slide. θ and θ_1 are related by Snell's law,

$$n_{air}\sin\theta=n_g\sin\theta_1 \tag{3}$$

where n_g is the refractive index of the glass slide. The complex amplitude $U(x,y,d_1)$ inside the first glass slide is now proportional to $\exp(-jk_1r)=\exp(-jk_1(d_1\cos\theta_1+x_1\sin\theta_1))$.

So that the complex amplitude transmittance of the first glass slide is:

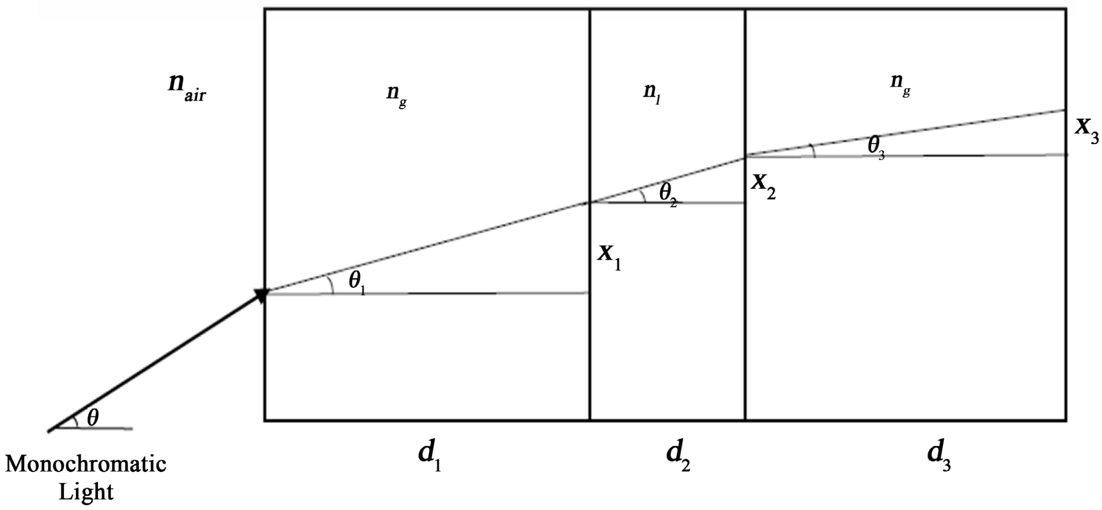

Figure 1. Propagation of the incident plane wave through the system of two glass slides and liquid in between.

$$t_1(x,y)=\exp\left(-jk_1\left(d_1\cos\theta_1+x_1\sin\theta_1\right)\right) \tag{4}$$

Equation (4) can be putted in the form,

$$t_1(x,y)=\exp\left(-jk_1\left(d_1-\frac{1}{2}d_1\left(\frac{\theta}{n_g}\right)^2+x_1\left(\frac{\theta}{n_g}\right)\right)\right) \tag{5}$$

From **Figure 1**, $\tan x_1=d_1\tan\theta_1$, $\tan\theta_1\approx\theta_1\approx\frac{\theta}{n_g}$ *i.e.* $x_1=d_1\left(\frac{\theta}{n_g}\right)$

By substitution in Equation (5),

$$t_1(x,y)=\exp\left(-jk_1\left(d_1-\frac{1}{2}d_1\left(\frac{\theta}{n_g}\right)^2+d_1\left(\frac{\theta}{n_g}\right)^2\right)\right) \tag{6}$$

$$i.e.\ \ t_1(x,y)=\exp\left(-jk_1\left(d_1\right)\right)\exp\left(-jk_1\left(\frac{d_1\theta^2}{2n_g^2}\right)\right) \tag{7}$$

For the second transmission, from the first glass slide medium to the liquid medium, and by using Snell's law,

$$n_g\sin\theta_1=n_l\sin\theta_2 \tag{8}$$

So that the complex amplitude transmittance of the liquid medium is:

$$t_2(x,y)=\exp\left(-jk_2\left(d_2\cos\theta_2+x_2\sin\theta_2\right)\right) \tag{9}$$

Equation (9) can be putted in the form,

$$t_2(x,y)=\exp\left(-jk_2\left(d_2\left(1-\frac{1}{2}\theta_2^2\right)+d_2\frac{\theta_1}{n_l}\theta_2\right)\right) \tag{10}$$

$$i.e.\ \ t_2(x,y)=\exp\left(-jk_2\left(d_2+\frac{1}{2}d_2\frac{\theta^2}{n_g^2n_\ell^2}\right)\right) \tag{11}$$

$$t_2(x,y)=\exp\left(-jk_2\left(d_2\right)\right)\exp\left(-jk_2d_2\left(\frac{1}{2}\frac{\theta^2}{n_g^2n_\ell^2}\right)\right) \tag{12}$$

For given the complex amplitude transmittance of the second glass slide, expresses the third transmission, from the liquid medium to the second glass slide.

$$t_3(x,y)=\exp\left(-jk_3\left(d_3\left(1-\frac{1}{2}\theta_3^2\right)+x_3\theta_3\right)\right) \tag{13}$$

So that $t_3(x,y)$ can be putted in the form:

$$t_3(x,y)=\exp\left(-jk_3\left(d_3+\frac{1}{2}d_3\left(\frac{\theta}{n_\ell n_g^2}\right)^2\right)\right),\ \text{or}$$

$$t_3(x,y)=\exp\left(-jk_3\left(d_3\right)\right)\exp\left(-jk_3\left(\frac{1}{2}d_3\frac{\theta^2}{n_\ell^2n_g^4}\right)\right) \tag{14}$$

The complex amplitude transmittance of the system of the two glass slides and the liquid:

$$t(x,y)=t_1(x,y)t_2(x,y)t_3(x,y) \tag{15}$$

By putting $k_1 \cong k_2 \cong k_3 \cong k$, and from Equations (7), (12), and (14)

$$t(x,y)=\exp\left(-jk\left(d_1+d_2+d_3\right)\right) \tag{16}$$

$$\begin{aligned} t(x,y) &= \exp\left(-jk_1(d_1)\right)\exp\left(-jk_1\left(\frac{d_1\theta^2}{2n_g^2}\right)\right)\exp\left(-jk_2(d_2)\right) \\ &\cdot\exp\left(-jk_2 d_2\left(\frac{1}{2}\frac{\theta^2}{n_g^2 n_\ell^2}\right)\right)\exp\left(-jk_3(d_3)\right)\exp\left(-jk_3\left(\frac{1}{2}d_3\frac{\theta^2}{n_\ell^2 n_g^4}\right)\right) \end{aligned} \tag{17}$$

The amplitude distribution $A_2(x,y)$ after the second exposure, which can be obtained with an angle of incidence θ of the plane wave and observed in the observation plane and given as:

$$\begin{aligned} A_2(x,y) &= \frac{1}{j\lambda z}ae^{i\phi}e^{jkz}\exp\left(-jk_1(d_1)\right)\exp\left(-jk_1 d_1\left(\frac{\theta^2}{2n_g^2}\right)\right)\exp\left(-jk_2(d_2)\right) \\ &\cdot\exp\left(-jk_2 d_2\left(\frac{1}{2}\frac{\theta^2}{n_g^2 n_\ell^2}\right)\right)\exp\left(-jk_3(d_3)\right)\exp\left(-jk_3 d_3\left(\frac{1}{2}\frac{\theta^2}{n_\ell^2 n_g^4}\right)\right) \\ &\cdot e^{\frac{j\pi}{\lambda z}\left(x^2+y^2\right)}\exp\left(j2\pi\Delta\xi\omega_x\right)F\left\{A(\xi,\eta)\right\} \end{aligned} \tag{18}$$

$$\begin{aligned} A_2(x,y) &= \frac{1}{j\lambda z}ae^{i\phi}e^{jkz}\exp\left(-jk_1(d_1)\left(1+\frac{\theta^2}{2n_g^2}\right)\right)\exp\left(-jk_2(d_2)\left(1+\frac{1}{2}\frac{\theta^2}{n_g^2 n_\ell^2}\right)\right) \\ &\cdot\exp\left(-jk_3(d_3)\left(1+\frac{1}{2}\frac{\theta^2}{n_\ell^2 n_g^4}\right)\right)e^{\frac{j\pi}{\lambda z}\left(x^2+y^2\right)}\exp\left(j2\pi\Delta\xi\omega_x\right)F\left\{A(\xi,\eta)\right\} \end{aligned} \tag{19}$$

By adding the two Equations (2) and (19), the intensity distribution in the observation plane can be written as,

$$\begin{aligned} I &= \left(\frac{1}{\lambda z}\right)^2 F^2\left\{A(\xi,\eta)\right\}\left(2+2\cos\left(2\pi\Delta\xi\omega_x - kd_1\frac{\theta^2}{2n_g^2}\right.\right. \\ &\left.\left. -kd_2\frac{\theta^2}{2n_g^2 n_\ell^2} - kd_3\frac{\theta^2}{2n_\ell^2 n_g^4}\right)\right) \end{aligned} \tag{20}$$

At maximum intensity, and where $m = 1$,

$$2\pi\Delta\xi\omega_x - kd_1\frac{\theta^2}{2n_g^2} - kd_2\frac{\theta^2}{2n_g^2 n_\ell^2} - kd_3\frac{\theta^2}{2n_\ell^2 n_g^4} = 2m\pi \tag{21}$$

From equation (21), we can get a new equation for given the refractive index of a liquid,

$$n_\ell = \sqrt{\frac{\frac{d_2}{\lambda}\frac{\theta^2}{2n_g^2}+\frac{d_3}{\lambda}\frac{\theta^2}{2n}}{\Delta\xi\omega_x - \frac{d_1}{\lambda}\left(\frac{\theta^2}{2n_g^2}-1\right)}} \tag{22}$$

where $\omega_x = \frac{2\pi}{\lambda_x}$, and $\Delta\xi = M\xi_m = \frac{\lambda z}{\lambda_x}$, M is the magnification of the imaging system, and ξ_m is the mechanical displacement used for the calibration of the system [10] [11].

Equation (22) can be putted in the form,

$$n_\ell = \sqrt{\frac{\theta^2\left(d_2 + \frac{d_3}{n_g^2}\right)}{2\lambda n_g^2\left(2\pi\frac{\lambda z}{\lambda_x^2} - \frac{d_1}{\lambda}\frac{\theta^2}{2n_g^2} - 1\right)}} \tag{23}$$

Using Equation (23), we can get a formula for getting the fringe spacing λ_x,

$$\lambda_x = \sqrt{\frac{2\pi\lambda z}{\frac{\theta^2\left(d_2 + d_3/n_g^2\right)}{2\lambda n_g^2 n_\ell^2} + \frac{d_1}{\lambda}\frac{\theta^2}{2n_g^2} + 1}} \tag{24}$$

Java-based image processing program was used for the calculation of the fringe spacing of the computer simulation results for given the refractive index.

3. Computer Simulation Results and Discussions

Figure 2 shows illustration of computer simulation for observation of correlation fringes in the spectral field for Zamzam, bottled and distilled waters. The illustration of the optical configuration is implemented to presents a comparative study of Zamzam, bottled drinking and distilled waters by a novel computer simulation speckle photography method using Fourier transform. The system of the two lass slides and the liquid is illuminated with a coherent laser beam with six discrete wavelengths across the visible spectrum (λ = 632.8 nm, 589.3 nm, 577.0 nm, 546.1 nm, 435.8 nm, and 404.7 nm respectively). The thicknesses of the two glass slides are $d_1 = 300\ \mu\text{m}$ and $d_3 = 300\ \mu\text{m}$ respectively, also the thickness of the liquid is $d_2 = 250\ \mu\text{m}$.

The spatially coherent light transmitted through the glass plate illuminates a rough surface, the laser beam spot at the diffuser plane was kept 2 cm in diameter to ensure suitable speckle size. The distance between the rough surface and the imaging plane was Z = 95 cm.

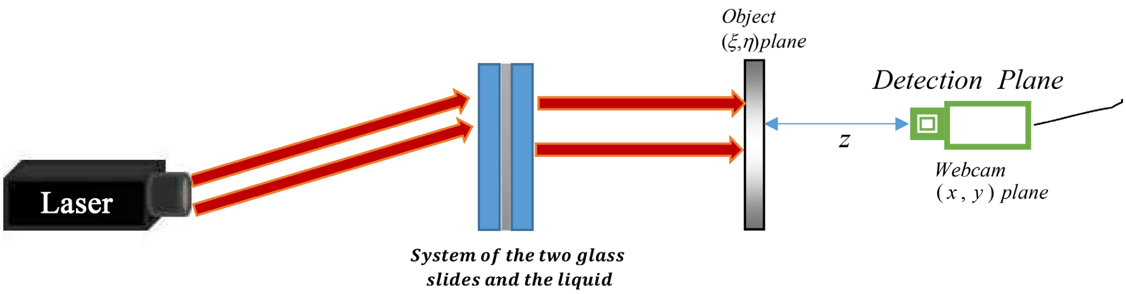

Figure 2. Illustration of computer simulation for observation of correlation fringes in the spectral field for Zamzam, bottled drinking and distilled waters.

If a rotation and non rotation given to the incident laser beam, the transmitted beam falls on the rough surface, resulting two images on the observation plane (CDD plane), which are combined digitally to give the correlation fringes.

Figures 3(a)-(d), **Figures 4(a)-(d)**, and **Figures 5(a)-(d)** show the images of correlation fringes in the spectral field for Zamzam, bottled drinking and distilled waters at wavelengths 0.6328 μm, 0.5461 μm, and 0.4047 μm respectively. The rotation angle of the incident laser beam was $\theta = 0.1^{\circ}$. The distance between the rough surface and the observation plane Z was 95 cm. From these correlation fringes, we can observe that the degree of visibility of the correlation fringes is clearer in the case of Zamzam water than the other waters even with a wavelength change. From the intensity distribution of the obtained correlation fringes, we can get the fringe spacing λ_x, which can be substituted in Equation (23) to get the refractive index of the liquid. As we can see from the figures, the fringe spacing decreases with decreasing the wavelengths of the used light. Also the fringe spacing decreases with increasing the refractive index of the liquid (Zamzam, bottled drinking and distilled waters, respectively). This explains the superiority of the visibility of the correlation fringes in case of Zamzam water.

4. Measurement Uncertainties of Method

The uncertainty of the refractive index n_ℓ was estimated by combining the standard uncertainties of the parameters $\theta, \lambda, d_1, d_2, d_3, \lambda_x$, and z.The relation between the value of n_ℓ and input parameters can be expressed by a model:

$$n_\ell = f\left(\theta, \lambda, d_1, d_2, d_3, \lambda_x, z\right) \tag{25}$$

where $\theta, \lambda, d_1, d_2, d_3, \lambda_x$ and z represent model input parameters. The uncertainty of the results $u\left(n_\ell\right)$ depends on the uncertainty of the input parameters, and can be described by the equation

$$u\left(n_\ell\right)^2 = \sum_{i=1}^{N}\left(\frac{\partial n_\ell}{\partial y_i}\right)^2 u\left(y_i\right)^2 \tag{26}$$

$$\begin{aligned} u\left(n_\ell\right)^2 = {} & \left(\frac{\partial n_\ell}{\partial \theta}\right)^2 u(\theta)^2 + \left(\frac{\partial n_\ell}{\partial \lambda}\right)^2 u(\lambda)^2 + \left(\frac{\partial n_\ell}{\partial d_1}\right)^2 u\left(d_1\right)^2 + \left(\frac{\partial n_\ell}{\partial d_2}\right)^2 u\left(d_2\right)^2 \\ & + \left(\frac{\partial n_\ell}{\partial d_3}\right)^2 u\left(d_3\right)^2 + \left(\frac{\partial n_\ell}{\partial \lambda_x}\right)^2 u\left(\lambda_x\right)^2 + \left(\frac{\partial n_\ell}{\partial z}\right)^2 u(z)^2 \end{aligned} \tag{27}$$

where $y_1, \cdots, y_i, \cdots, y_N$ represent model input parameters, $u\left(y_i\right)\left(u(\theta), u(\lambda), u\left(d_1\right), u\left(d_2\right), u\left(d_3\right), u\left(\lambda_x\right), u(z)\right)$ are the standard uncertainties of the input parameters, and $\frac{\partial n_\ell}{\partial y_i}$ is a sensitivity coefficient. The sensitivity coefficient describes how the measurement result varies with changes in the value of input estimates. Equation (26) is valid for measurement where there is no correlation between input parameters.

Depending on the formulae (23) of the refractive index and also on equation (27), $\frac{\partial n_\ell}{\partial y_i}$ can be expressed in the form:

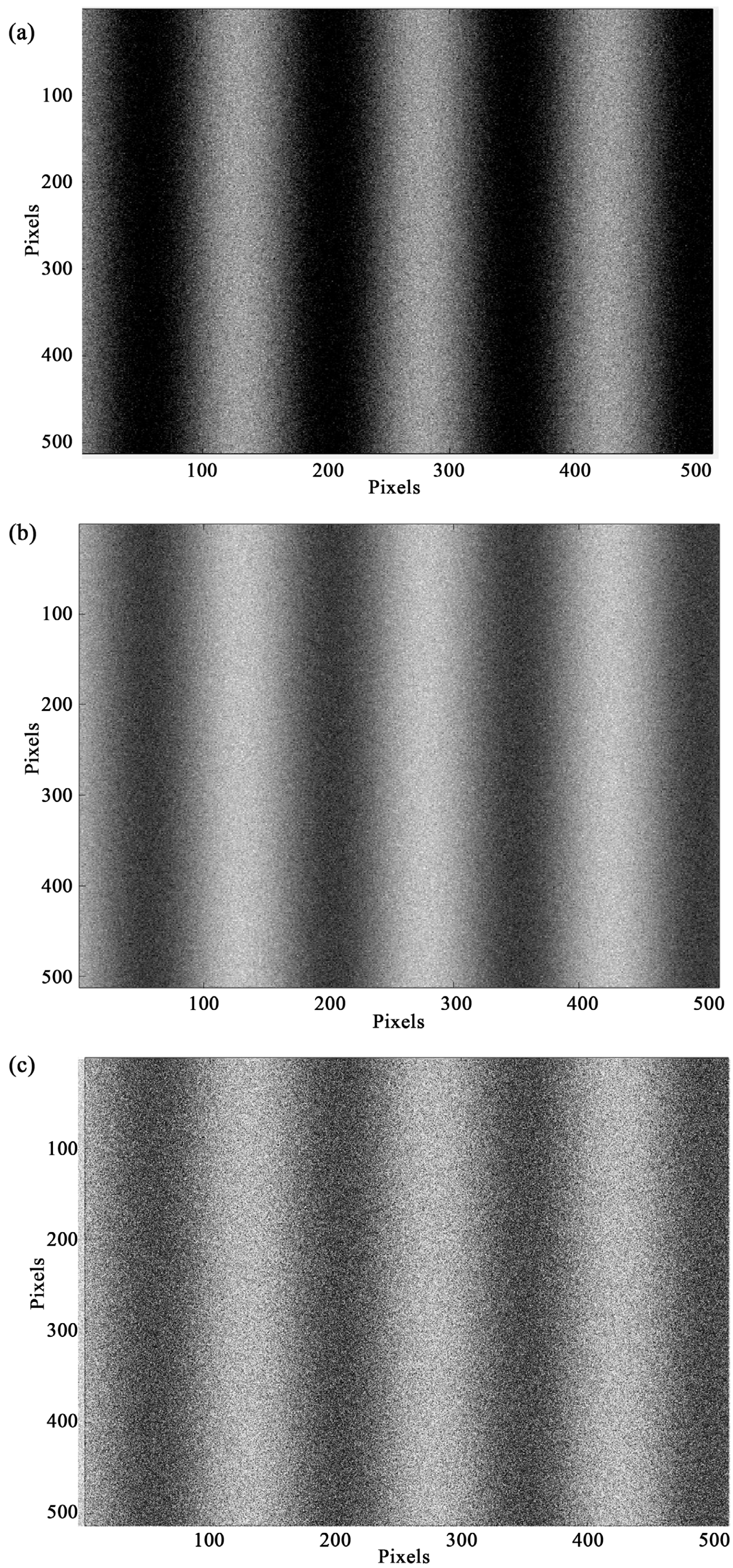

Figure 3. Images of correlation fringes in the spectral field for Zamzam, bottled drinking and distilled waters respectively. The rotation angle was $\theta = 0.1^{\circ}$ at wavelength 0.6328 μm. The distance between the rough surface and the observation plane Z was 95 cm.

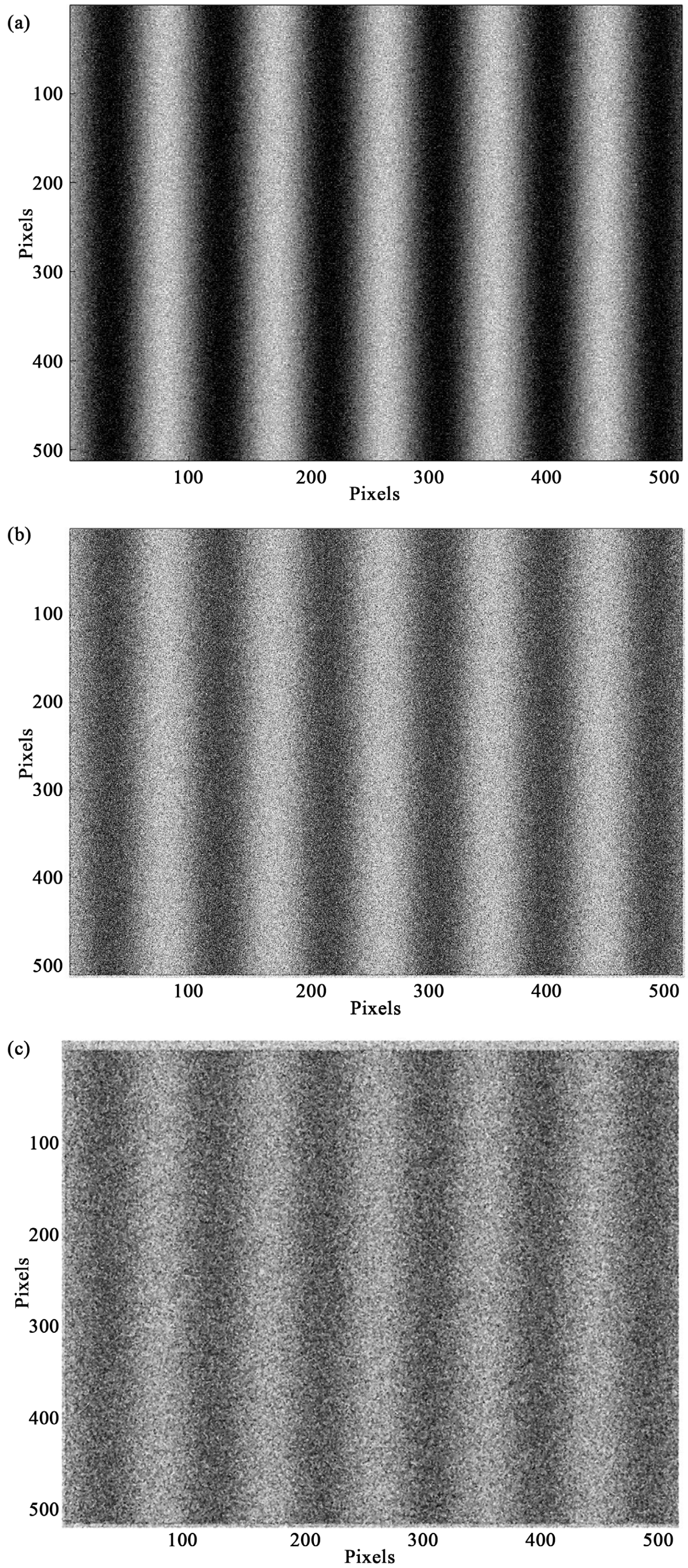

Figure 4. Images of correlation fringes in the spectral field for Zamzam, bottled drinking and distilled waters respectively. The rotation angle was $\theta = 0.1^{\circ}$ at wavelength 0.5461 μm. The distance between the rough surface and the observation plane Z was 95 cm.

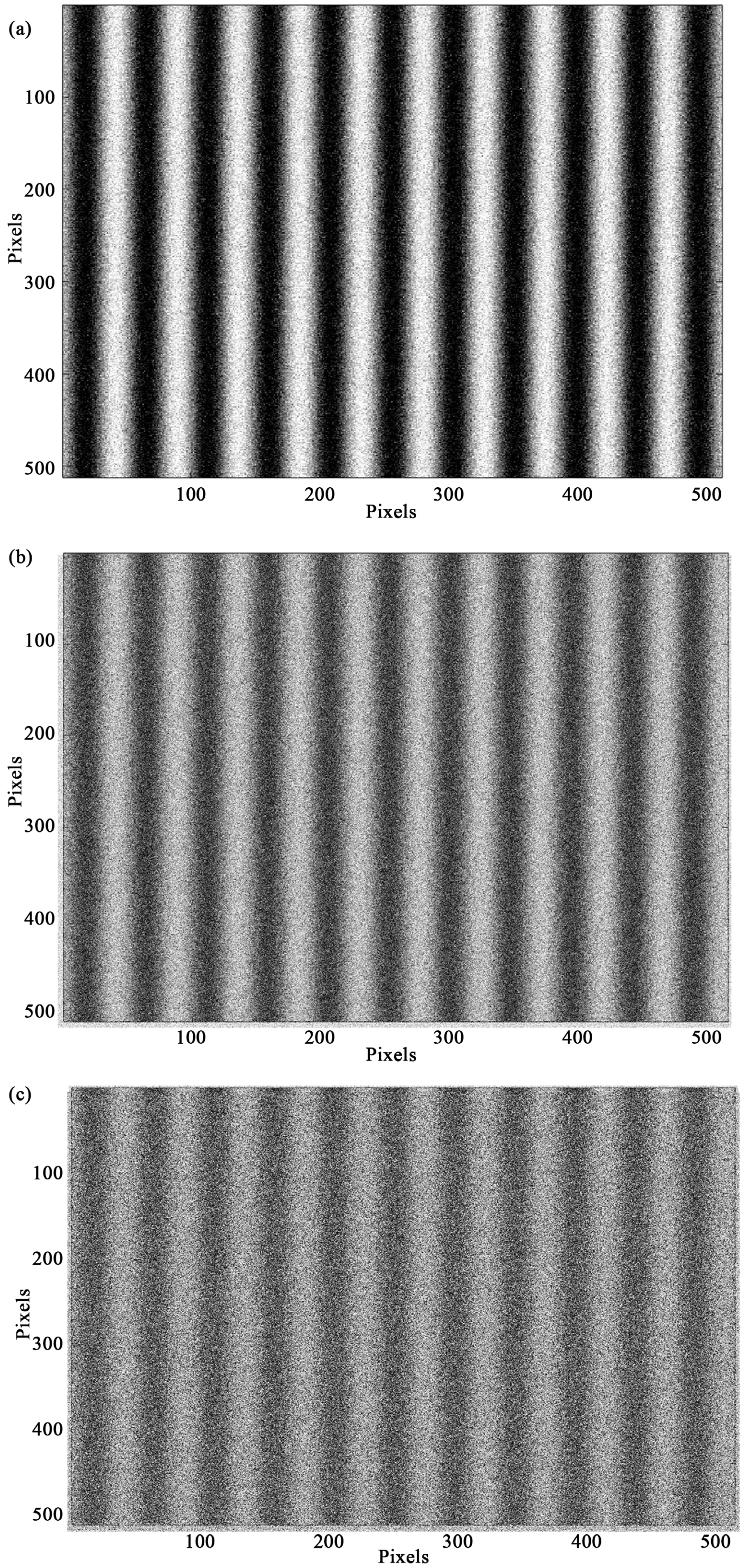

Figure 5. Images of correlation fringes in the spectral field for Zamzam, bottled drinking and distilled waters respectively. The rotation angle was $\theta = 0.1^{\circ}$ at wavelength 0.4047 μm. The distance between the rough surface and the observation plane Z was 95 cm.

$$\frac{\partial n_\ell}{\partial \theta}=\frac{\left[\left(d_2+d_3/n_g^2\right)/2\lambda n_g^2\right]^{1/2}\left(1-2\pi\frac{\lambda Z}{\lambda_x^2}\right)}{\theta^3\left[2\pi\frac{\lambda Z}{\lambda_x^2}\frac{1}{\theta^2}-\frac{d_1}{2\lambda n_g^2}-\frac{1}{\theta^2}\right]^{-3/2}}, \tag{28}$$

$$\frac{\partial n_\ell}{\partial \lambda}=\frac{-1}{2}\frac{\left[\theta^2\left(d_2+d_3/n_g^2\right)/2n_g^2\right]^{1/2}\left(4\pi\frac{\lambda Z}{\lambda_x^2}-1\right)}{\left[2\pi\frac{\lambda^2 Z}{\lambda_x^2}-\frac{d_1\theta^2}{2n_g^2}-\lambda\right]^{3/2}} \tag{29}$$

$$\frac{\partial n_\ell}{\partial \lambda_x}=\frac{\left[\theta^2\left(d_2+d_3/n_g^2\right)/2\lambda n_g^2\right]^{1/2}\left(2\pi\frac{\lambda Z}{\lambda_x^3}\right)}{\left[2\pi\frac{\lambda Z}{\lambda_x^2}-\frac{d_1\theta^2}{2\lambda n_g^2}-1\right]^{3/2}} \tag{30}$$

$$\frac{\partial n_\ell}{\partial d_1}=\frac{\theta^2}{4\lambda n_g^2}\frac{\left[\theta^2\left(d_2+d_3/n_g^2\right)/2\lambda n_g^2\right]^{1/2}}{\left[2\pi\frac{\lambda Z}{\lambda_x^2}-\frac{d_1\theta^2}{2\lambda n_g^2}-1\right]^{3/2}} \tag{31}$$

$$\frac{\partial n_\ell}{\partial d_2}=\frac{1}{2}\frac{\left[\theta^2/2\lambda n_g^2\right]^{1/2}}{\left(d_2+\frac{d_3}{n_g^2}\right)^{1/2}\left[2\pi\frac{\lambda Z}{\lambda_x^2}-\frac{d_1\theta^2}{2\lambda n_g^2}-1\right]^{1/2}} \tag{32}$$

$$\frac{\partial n_\ell}{\partial d_3}=\frac{1}{2}\frac{\left(1/n_g^2\right)\left[\theta^2/2\lambda n_g^2\right]^{1/2}}{\left(d_2+\frac{d_3}{n_g^2}\right)^{1/2}\left[2\pi\frac{\lambda Z}{\lambda_x^2}-\frac{d_1\theta^2}{2\lambda n_g^2}-1\right]^{1/2}} \tag{33}$$

and

$$\frac{\partial n_\ell}{\partial z}=\frac{-1}{2}\frac{\left[\theta^2\left(d_2+d_3/n_g^2\right)/2\lambda n_g^2\right]^{1/2}\left(2\pi\frac{\lambda}{\lambda_x^2}\right)}{\left[2\pi\frac{\lambda Z}{\lambda_x^2}-\frac{d_1\theta^2}{2\lambda n_g^2}-1\right]^{3/2}} \tag{34}$$

where $\frac{\partial n_\ell}{\partial \theta}$, $\frac{\partial n_\ell}{\partial \lambda}$, $\frac{\partial n_\ell}{\partial \lambda_x}$, $\frac{\partial n_\ell}{\partial d_1}$, $\frac{\partial n_\ell}{\partial d_2}$, $\frac{\partial n_\ell}{\partial d_3}$, and $\frac{\partial n_\ell}{\partial z}$ are the sensitivity coefficient of the angle of incidence of the coherent light beam, the sensitivity coefficient of the wavelength of the used light, the sensitivity coefficient of the fringe spacing, the sensitivity coefficient of the thickness of the first glass slide, the sensitivity coefficient of the thickness of the liquid putted between the two slides, the sensitivity coefficient of the thickness of the second glass slide, the sensitivity coefficient of the distance between the rough surface and the observation plane CCD.

Relative uncertainty contributions are used to illustrate the relative impact of different uncertainty components. The relative contribution (r_i) of an uncertainty component y_i, to the combined standard uncertainty is defined here as

$$r_i = \frac{\partial n_\ell / \partial y_i}{u(n_\ell)^2} u(y_i)^2 \tag{35}$$

where n_ℓ is the model equation $\left(n_\ell = f\left(y_1, y_2, \cdots, y_i, \cdots, y_N\right)\right)$, y_i are the input parameters $(\theta, \lambda, d_1, d_2, d_3, \lambda_x, z)$, and $u(n_\ell)^2$ is the combined uncertainty calculated according to Equation (25).

Figure 6 shows the relation between the refractive index n_ℓ of the Zamzam, bottled drinking, and distilled waters and the six discrete wavelengths across the visible spectrum. From that figure, we can conclude that the values of the refractive index for the different waters are very close together with increasing the wavelength of the used light, and getting away from each other with decreasing the values of the wavelengths.

Figure 7 Dependence of the combined uncertainty of the refractive index n_ℓ of Zamzam, bottled drinking and distilled waters on changing the value of the angle of incidence of the coherent light beam at different values of refractive index.

The values of Z = 95 cm, d_1 = 300 µm, d_2= 250 µm, and d_3= 300 µm are constant during the simulation. The figure concluded that the combined uncertainty of the refractive index for the different waters somewhat close together in case of shortest refractive index, and getting away much more from each other in case largest refractive index.

Figure 8 shows the dependence of the combined uncertainty of the refractive index n_ℓ of Zamzam, bottled drinking, and distilled waters on changing the value of the angle of incidence of the coherent light beam at six discrete wavelengths across the visible spectrum.

The figure concluded that the combined uncertainty of the refractive index for

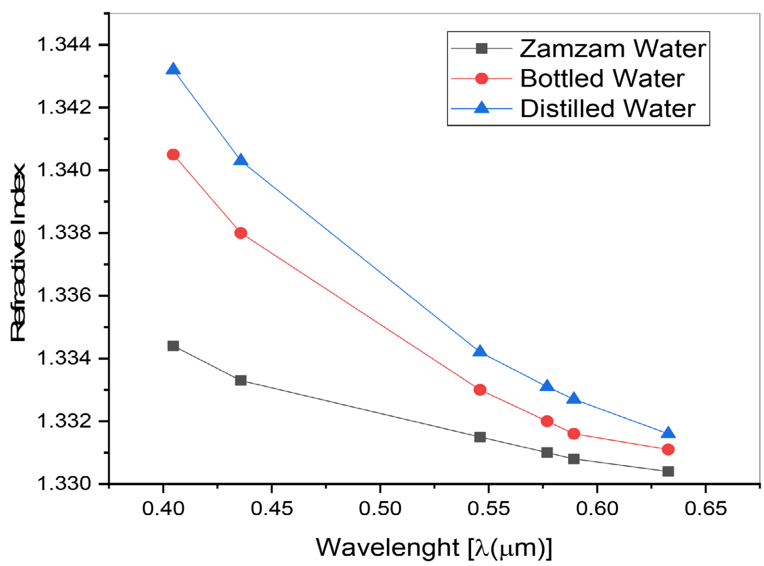

Figure 6. Relation between the refractive index n_ℓ of the Zamzam, bottled drinking and distilled waters and the six discrete wavelengths across the visible spectrum.

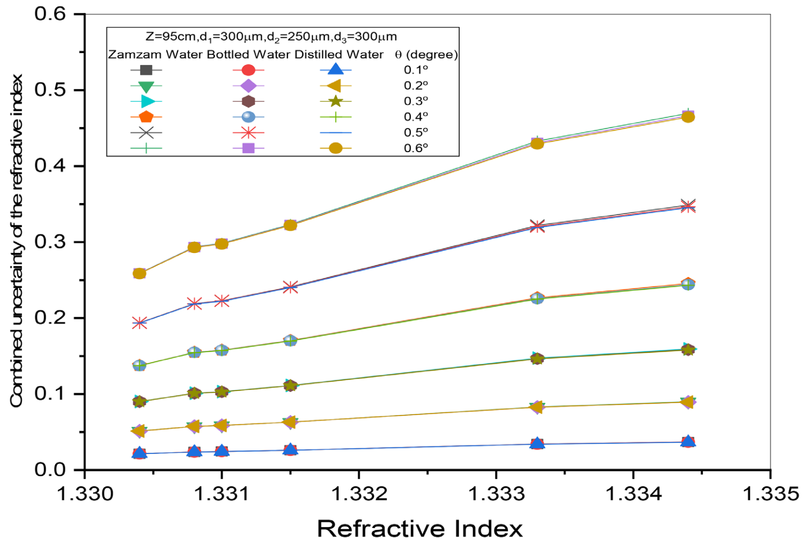

Figure 7. Dependence of the combined uncertainty of the refractive index n_ℓ of Zamzam, bottled drinking and distilled waters on changing the value of the angle of incidence of the coherent light beam at different values of refractive index.

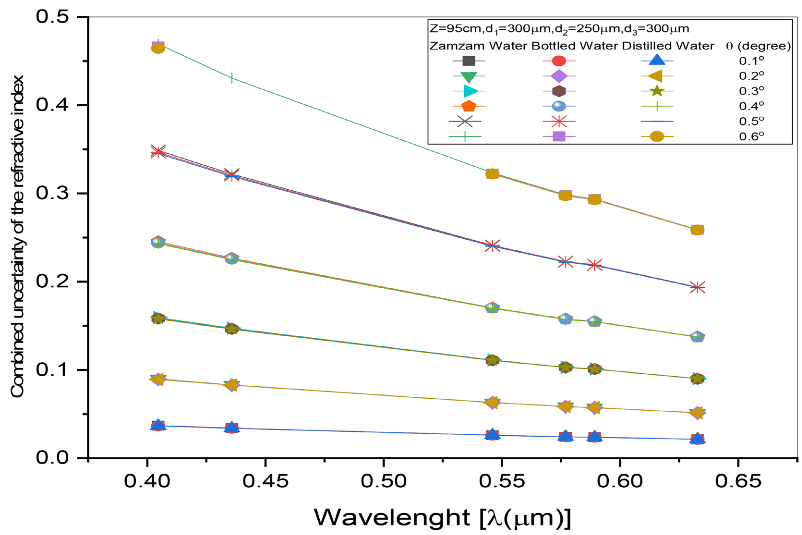

Figure 8. Dependence of the combined uncertainty of the refractive index n_ℓ of Zamzam, bottled drinking, and distilled waters on changing the value of the angle of incidence of the coherent light beam at six discrete wavelengths across the visible spectrum.

the different waters somewhat close together in case of longest wavelength, and getting away much more from each other in case shortest wavelength.

Figure 9 shows the dependence of the the relative uncertainty of the fringe spacing λ_x of the Zamzam, bottled drinking and distilled waters and the value of the discrete wavelengths across the visible spectrum at different angle of incidence of the coherent light beam.

From that figure, we can conclude that the relative uncertainty contribution of λ_x ($r_{\lambda_x} = \frac{\partial n_\ell / \partial \lambda_x}{u(n_\ell)^2} u(\lambda_x)^2$) approximately have the same value for different values of wavelengths at the small values of the angle of incidence of the coherent light beam. When the angle of incidence θ increases, the relative uncertainty contribution of λ_x increases, too.

Figure 10 shows the dependence of the relative uncertainty of the used wavelength λ and the value of the discrete wavelengths across the visible spectrum at different angle of incidence of the coherent light beam for the Zamzam, bottled

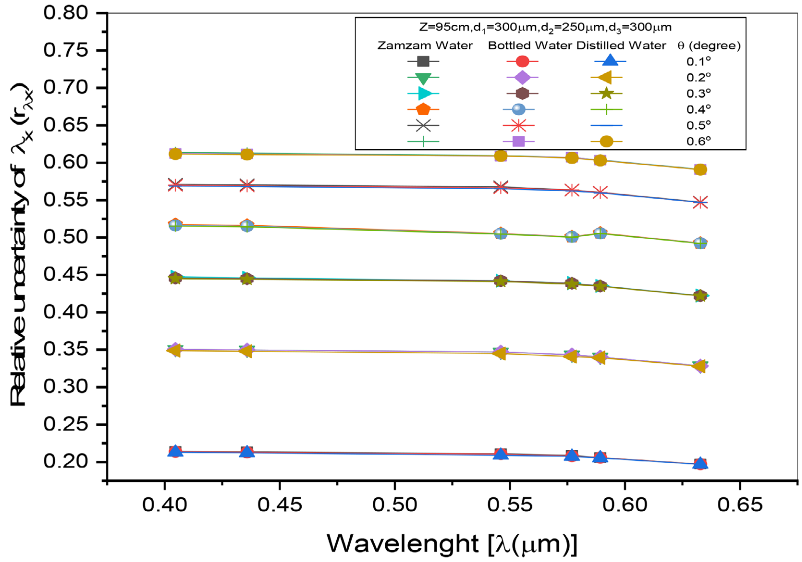

Figure 9. Relation between the relative uncertainty of the fringe spacing λ_x of the Zamzam, bottled drinking and distilled waters and the value of the discrete wavelengths across the visible spectrum at different angle of incidence of the coherent light beam.

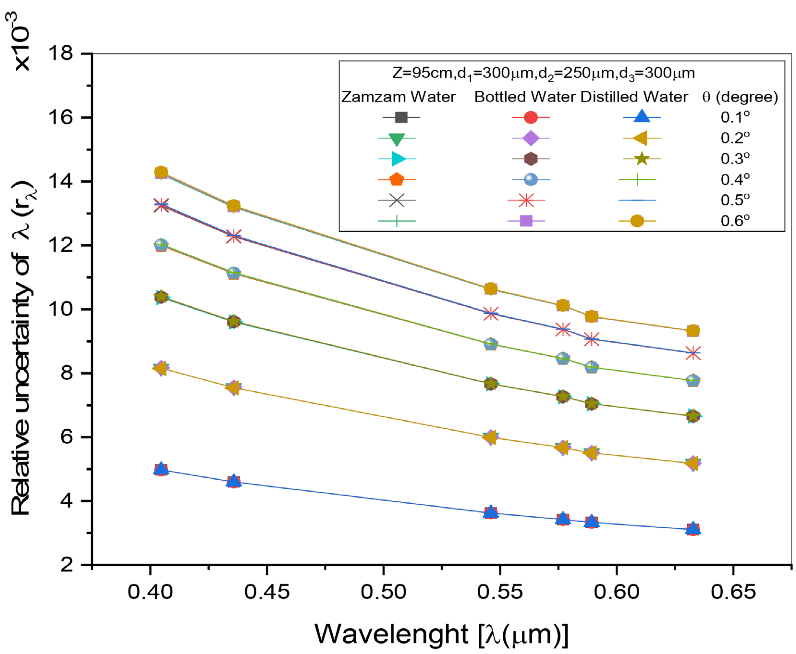

Figure 10. Relation between the relative uncertainty of the used wavelength λ and the value of the discrete wavelengths across the visible spectrum at different angle of incidence of the coherent light beam for the Zamzam, bottled drinking, and distilled waters.

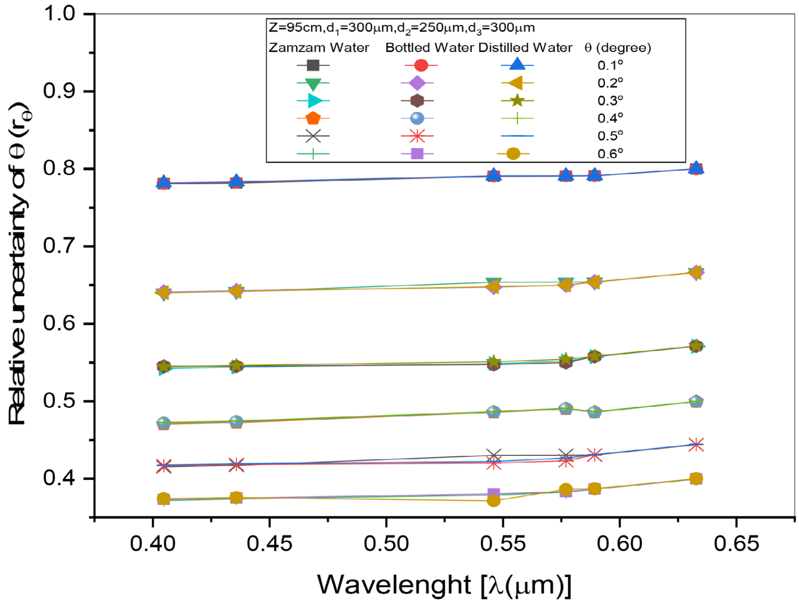

Figure 11. Relation between the relative uncertainty of the used angle of incidence θ and the value of the discrete wavelengths across the visible spectrum at different angle of incidence of the coherent light beam for the Zamzam, bottled drinking, and distilled waters.

drinking, and distilled waters.

It can show that the values of the relative uncertainty contribution of the wavelength ($r_\lambda = \frac{\partial n_\ell / \partial \lambda}{u(n_\ell)^2} u(\lambda)^2$) getting away from each other with increasing the values of the wavelengths and also the angle of incidence of the coherent light beam.

Figure 11 shows the dependence of the relative uncertainty contribution of the angle of the incidence of the coherent light $r_\theta = \frac{\partial n_\ell / \partial \theta}{u(n_\ell)^2} u(\theta)^2$ on the discrete wavelengths across the visible spectrum at different angle of incidence of the light beam.

When the values of the wavelengths increase and also the angle of incidence of the light beam, the values of r_θ increases, too. The values of r_θ are approximately close with the same value for different values of the discrete wavelengths.

5. Conclusion

We have presented a simple computer simulation speckle technique for comparative study of Zamzam, bottled drinking and distilled waters. New theoretical formulae for the given refractive index were discovered to give a high documentation for the computer simulation work. Uncertainty of the refractive index measurements on wide range of changing the discrete wavelengths is given. It can be concluded that the computer simulation measurements of the refractive index are in good agreement with the theoretical new formulae, which also confirmed with the experimental results previously obtained. The degree of visibility of the correlation fringes is clearer in the case of Zamzam water than the other waters. The uses of laser light of wavelength 0.6328 μm and with a small angle of incidence 1˚, give the optimum combined uncertainty for given accurate measurement of the refractive index. It is concluded that Zamzam water has special and distinct optical refractive index that is different than those of bottled drinking and distilled waters.

Acknowledgements

This work is funded by grant number (12-NAN2287-10) from National Science Technology and Innovation Plan (NSTP), the King Abdul-Aziz City for Science and Technology (MAARIFH), Kingdom of Saudi Arabia. We thank the Science and Technology Unit at Umm Al-Qura University for their continuous logistic support.

Conflicts of Interest

The authors declare no conflicts of interest regarding the publication of this paper.

References

[1] Nascov, V., Samoilă, C. and Ursuțiu, D. (2013) Fast Computation Algorithms for Speckle. *AIP Conference Proceedings*, **1564**, 217. https://doi.org/10.1063/1.4832821

[2] Fujii, H., Uozumi, J. and Asakura, T. (1976) Computer Simulation Study of Image Speckle Patterns with Relation to Object Surface Profile. *Journal of the Optical Society of America*, **66**, 1222-1236. https://doi.org/10.1364/JOSA.66.001222

[3] Fujii, H., Asaku, J. and Shindo, Y. (1976) Measurement of Surface Roughness Properties by Using Image Speckle Contrast. *Journal of the Optical Society of America*, **66**, 1217-1222. https://doi.org/10.1364/JOSA.66.001217

[4] Chandra, B.P. and Bhaiya, (1983) A Simple, Accurate Alternative to the Minimum Deviation Method of Determining the Refractive Index of Liquids. *American Journal of Physics*, **51**, 160-161. https://doi.org/10.1119/1.13314

[5] Jenkins, D.D. (1982) Refractive Indices of Solutions. *Physics Education*, **17**, 82. https://doi.org/10.1088/0031-9120/17/2/413

[6] Shojiro, N. (1992) Measurement of the Refractive Index of Liquid Using Laser Beam Displacement. *Applied Optics*, **31**, 6690-6694. https://doi.org/10.1364/AO.31.006690

[7] Boulay, R., Gagnon, R., Rochette, D., *et al.* (1984) Paper Sheet Moisture Measurements in the Far Infrared. *International Journal of Infrared and Millimeter Waves*, **5**, 1221-1234. https://doi.org/10.1007/BF01010048

[8] Bass, J.D. and Weidner, D.J. (1984) Method for Measuring the Refractive Index of Transparent Solids. *Review of Scientific Instruments*, **55**, 1569. https://doi.org/10.1063/1.1137611

[9] El-Zaiat, S.Y. (2007) Inherent Optical Properties of Zamzam Water in the Visible Spectrum: Dispersion Analysis. *Arabian Journal for Science and Engineering*, **32**, 172-180.

[10] Moustafa, N.A. (2013) Digital Processing of Speckle Photography to Measure Refractive Index of a Transparent Plate. *Australian Journal of Basic and Applied Sciences*, **7**, 187-193. https://doi.org/10.1117/12.2020374

[11] Moustafa, N.A. (2013) Active Speckle Photography Method Using Fourier Transform for Measuring the Thickness of a Transparent Plate. *International Journal of Physics and Research* (*IJPR*), **3**, 61-72.

[12] Moustafa, N.A. (1999) Comparative Measurement in Speckle Interferometry Interferometry Using Holographically Generated Reference Wave Using the Single Reference Beam Technique. *Optics Communications*, **172**, 9-16. https://doi.org/10.1016/S0030-4018(99)00415-0